International Journal of Science Engineering and Advance Technology

Power Quality Improvement For PV/Battery Hybrid System Using Fuzzy Logic Controlling Technique

Pavan Molleti1, B.D.S.Prasad2
1PG Scholar, Pydah College of Engineering, Kakinada, AP, India.
2Assistant Professor, Pydah College of Engineering, Kakinada, AP, India.

Abstract— power quality improvement for pv/battery hybrid system using fuzzy logic controlling technique has been presented this paper. The PV side cascaded boost DC-DC converter is controlled by P&O algorithm to extract the maximum power from the solar irradiation. The battery energy storage system (BESS) is regulated to balance the power between PV generation and utility grid. In this paper a modified Instantaneous symmetrical components theory has been presented to the μG-VSC in micro-grid applications (i) to feed the generated active power in proportional to irradiation levels into the grid (ii) compensation of the reactive power, (iii) load balancing and (iv) mitigation of current harmonics, thus enabling the grid to supply only sinusoidal current at unity power factor. A new fuzzy logic control technique is also proposed in this paper for the battery converter with DC link voltage regulation capability. The dynamic performance of battery is improved with fuzzy logic controller, and shows the better performance compared with conventional method. A model of a hybrid PV Energy Conversion System is designed in MATLAB/SIMULINK software to test the effectiveness of the proposed control strategies.

Index Terms—PV energy conversion system, high gain inte-grated cascaded boost dc-dc converter, instantaneous symmetrical components theory, battery energy storage system.

I. INTRODUCTION

The PV source is a nonlinear energy source and direct connection of load will not give optimum utilization of the PV system. In order to utilize the PV source optimally, it is necessary to provide an intermediate electronic controller in between source and load under all operating conditions. Using this electronic controller it is possible to operate the PV source at maximum power point (MPP), thus improving the energy efficiency of the PV system. Many control algorithms have been reported in the literature to track maximum power from the PV arrays, such as incremental conductance (INC), constant voltage (CV), and perturbation and observation (P&O).

The two algorithms often used to achieve maximum power point tracking are the P&O and INC methods. Many DC-DC converter topologies are available to track the MPP in PV generating system. Cascade connection of conventional converters provides wider conversion ratios. One of the major advantages of these converters is a high gain and low current ripple. However, this configuration has a drawback that the total efficiency may become low if the numbers of stages are high, owing to power losses in the switching devices.

A quadratic converter configuration is also available that uses single switch and achieves quadratic gain. An interesting attractive converter topology is a high gain integrated cascaded boost converter having n-converters connected in cascade using a single active switch. The instability caused by the cascade structure is avoided, when compared with the conventional cascade boost converter. This class of converters can be used only when the required number of stages is not very large, else the efficiency will be reduced. However, these classes of converters for PV applications are not reported in the technical literature.

Micro-grid power converters can be classified into
(i) grid-feeding,
(ii) grid-supporting, and
(iii) grid-forming power converters.

There are many control schemes reported in the literature such as synchronous reference theory, power balance theory, and direct current vector control, for control of μG-VSC in micro grid application. These algorithms require complex coordinate transformations. Compared to the control strategies mentioned above, the Instantaneous symmetrical component based control proposed in this paper for micro-grid applications is simple in formulation, avoids interpretation of

instantaneous reactive power and needs no complex transformations.

II. SYSTEM DESCRIPTION

The envisaged system consists of a PV/Battery hybrid system with the main grid connecting to non-linear and unbalanced loads at the PCC as shown in the Fig. 1. The photovoltaic system is modeled as nonlinear voltage sources. The PV array is connected to HGICB dc-dc converter and bidirectional battery converter is shown in Fig. 1, which are coupled at the dc side of a μG-VSC. The HGICB (high gain integrated cascaded boost) dc-dc converter is connected to the PV array works as MPPT controller and battery converter is used to regulate the power flow between dc and ac side of the system.

III. MODELING AND CONTROL

The MPPT algorithm for HGICB Converter, control approaches for battery converter and μG-VSC are discussed in the following sections.

A. PV Array Model

The mathematical model of PV system referred in [8] is used in this work.

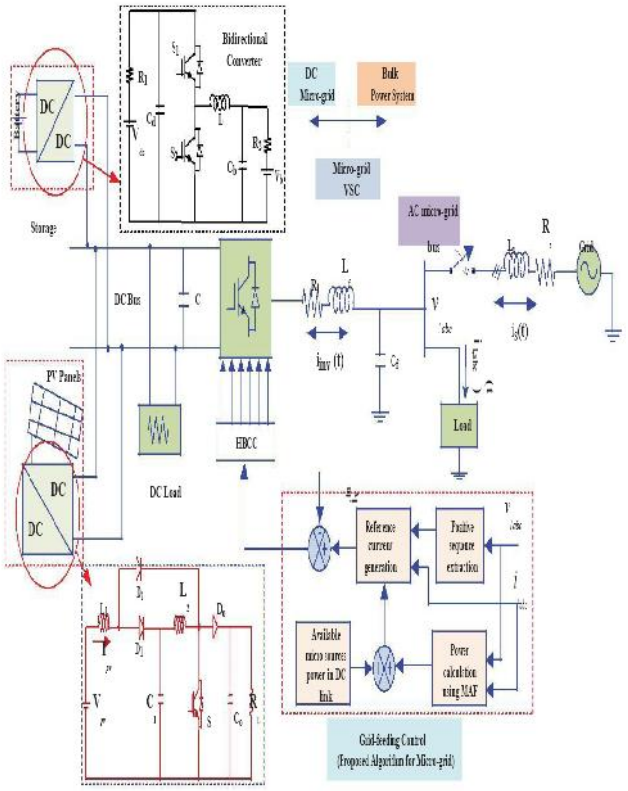

Fig. 1 Hybrid Energy Conversion System under consideration

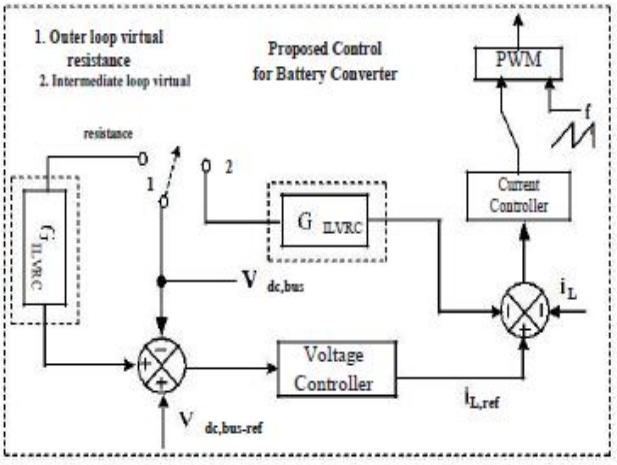

Fig. 2 A new modified control strategy for battery converter

B. Battery Converter Modeling

The battery converter goes through two topological stages in each switching period, its power stage dynamics can be described by a set of state equations. The average state space model of the converter can therefore be given as:

$$\frac{di_L}{dt} = \frac{v_{c1}\,d(t)}{L} - \frac{v_{c2}}{L} - \frac{(r_s + r_L)i_L}{L}$$

$$\frac{dv_{c1}}{dt} = \frac{v_{dc,Bus} - v_{c1}}{C_1 R1} - \frac{i_L\,d(t)}{C_1} \qquad (1)$$

$$\frac{dv_{c2}}{C_2} = \frac{v_B - v_{c2} - i_L\,dt}{C_2 R2}$$

The averaged model is nonlinear and time-invariant because of the duty cycle, $d(t)$. This model is finally linearized about the operating point to obtain a small-signal model is shown in Fig. 4. The following are the important transfer functions used to design the compensators and to analyze the system behavior under small signal conditions (i) the duty-cycle-to-output transfer function $Gcv(s)$, carries the information needed to determine the type of the voltage feedback compensation,(ii) the duty-cycle-to-inductor current transfer function $Gci(s)$, is needed to determine the current controller structure.

C. Proposed Control for Battery Converter

If AC side of μG-VSC has constant power appliances (CPAs), in the small-signal sense, CPAs nature leads to negative incremental input-conductance which causes destabilization of the dc-link voltage. On the micro-grid generation side, the inherent negative admittance

dynamics of their controlled conversion stages challenges the dc-link voltage control and stability. This effect is more with reduced dc-link capacitance. Therefore, in both cases, fast and effective control and stabilization of the dc-link voltage is very crucial issue. To address this problem, many methods are reported in the literature like (i) by large DC link capacitance (ii) by adding passive resistances at various positions in DC LC filter (iii) by loop cancellation methods.

In this paper, a new modified-ACMC (MACMC) control algorithm is proposed for effective control and stabilization of battery converter by introducing virtual resistance (VR) in the

(i) Outer loop called outer loop virtual resistance control (OLVRC)

(ii) Intermediate loop called inner loop virtual resistance control (ILVRC) as shown in Fig. 2. The proposed virtual resistance based dynamic damping methods aim at injecting a damping signal that compensate for negative conductance caused by CPAs without any power loss.

D. Design steps for Compensators of BESS

The effectiveness of proposed VRCs control algorithm is investigated and compared with the use of traditional ACMC. The flowchart for modes of operation of battery converter in grid feeding mode is shown in Fig. 3. The design guidelines for inner and outer loop compensators of ACMC are given below. The inner loop (current) gain can be written as:

$$T_i(s) = G_{id}(s)\, R_i\, G_{ci}(s)\, F_m \qquad (2)$$

The outer loop (voltage) gain can be written as:

$$T_v(s) = G_{vd}(s)\, G_{cv}(s)\, (1 + G_{ci}(s))\, F_m \qquad (3)$$

And the overall loop gain therefore can be written as:

$$T_1(s) = T_s + T_v \qquad (4)$$

Voltage Loop Design Steps:

i) Place one zero as high as possible, yet not exceeding resonating frequency of the converter.

ii) Place one pole at frequency of output capacitor ESR to cancel the effects of output capacitor ESR.

iii) Adjust, gain of compensator to trade-off stability margins and closed-loop performance.

iv) Another pole should be place at origin to boost the dc and low frequency gain of the voltage loop.

Similar steps mentioned above are followed to design current loop and for design of MACMC loops. Following the design procedure given above, the inner current and outer voltage loop compensators are designed to regulate the DC link voltage to 920 V.

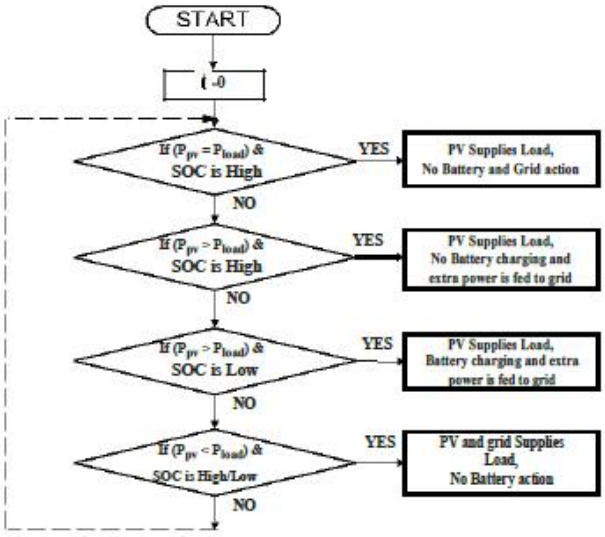

Fig. 3 Flow chart of power flow in hybrid system

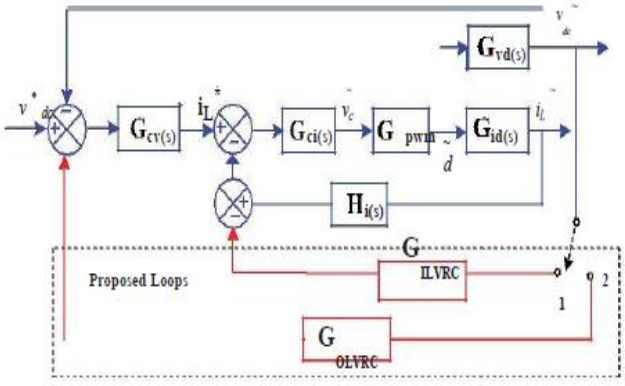

Fig. 4 Inner and outer loops of battery converter with MACMC

E. Generation of reference currents for μG-VSC

The main aim of the μG-VSC control is to cancel the effects of unbalanced and harmonic components of the local load, while supplying pre-specified amount of real and reactive powers to the load. Upon successfully meeting this objective, the grid current *ig* will then be balanced and so will be the PCC voltage *vp* provided, grid voltage *vg* is balanced. Let us denote the three phases by the subscripts a, b and c. Since *ig* is balanced, we can write:

$$i_{ga} + i_{gb} + i_{gc} = 0 \,. \qquad (5)$$

From the Fig. 1, Kirchhoff's current law (KCL) at PCC gives

$$i_{g,abc} + i_{inv,abc} = i_{L,abc} \,. \qquad (6)$$

Therefore, from (5) and (6), we can write as:

$$i_{inv,a} + i_{inv,b} + i_{inv,c} = i_{L,a} + i_{L,b} + i_{L,c} \,. \qquad (7)$$

Since *ig* is balanced due to the action of the compensator, the voltage *vp* will also become balanced. Hence, the instantaneous real powers *Pg* will be equal to its average component. Therefore, we can write

$$P_g = v_{pa}\, i_{ga} + v_{pb}\, i_{gb} + v_{pc}\, i_{gc} \qquad (8)$$

Solving above equations, the μG-VSC reference currents are obtained as follows:

$$i^*_{inv,a} = i_{la} - \frac{v_{ga} + \beta(v_{gb} - v_{gc})}{} (P_{lavg} - P_{\mu s} + P_{loss})$$

$$i^*_{inv,b} = i_{lb} - \frac{v_{gb} + \beta(v_{gc} - v_{ga})}{} (P_{lavg} - P_{\mu s} + P_{loss})$$

$$i^*_{inv,c} = i_{lc} - \frac{v_{gc} + \beta(v_{ga} - v_{gb})}{} (P_{lavg} - P_{\mu s} + P_{loss}) \qquad (9)$$

And $Qs = Ql - Q_{\mu s}$, and by substituting β $Ps = \sqrt{3}Qs$ into the equation (9), the modified G-VSC reference current equations in terms of active and reactive components are obtained as:

$$i^*_{inv,a} = i_{la} - \frac{v_{ga} P_s}{\sum_{j=a,b,c} v_{gj}^2} - \frac{(v_{gb} - v_{gc})\, Q_s}{\sqrt{3} \sum_{j=a,b,c} v_{gj}^2}$$

$$i^*_{inv,b} = i_{lb} - \frac{v_{gb} P_s}{\sum_{j=a,b,c} v_{gj}^2} - \frac{(v_{gc} - v_{ga})\, Q_s}{\sqrt{3} \sum_{j=a,b,c} v_{gj}^2}$$

$$i^*_{inv,c} = i_{lc} - \frac{v_{gc} P_s}{\sum_{j=a,b,c} v_{gj}^2} - \frac{(v_{ga} - v_{gb})\, Q_s}{\sqrt{3} \sum_{j=a,b,c} v_{gj}^2} \qquad (10)$$

In equations (9) and (10), $P_{\mu s}$, *Plavg* , and *Ql* are the available micro source power, average load power, and load reactive power respectively. *Ploss* denotes the switching losses and ohmic losses in actual compensator. The term *Plavg* is obtained using a moving average filter of one cycle window of time *T* in seconds.

TABLE I
SYSTEM PARAMETERS

System Quantities	Values
System voltages	325 V peak phase to neutral, 50 Hz
Linear Load	$Z_{la} = 50 + j1.57\ \Omega$, $Z_{lb} = 45 + j3.14\ \Omega$, $Z_{lc} = 40 + j4.71\ \Omega$
Non-Linear Load	Three phase full bridge rectifier load feeding a R-L load of 44Ω-3 mH
G-VSC parameters	C_{dc}=660 μF, V_{dcref}=920 V, L_f= 5 mH, R_f= 0.1Ω
Hysteresis band	0.25 A

IV. SIMULATION RESULTS

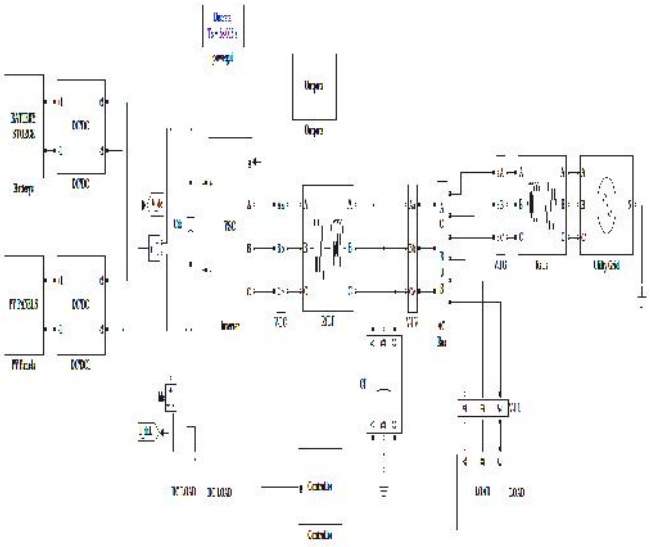

Fig 5 simulation diagram of proposed system

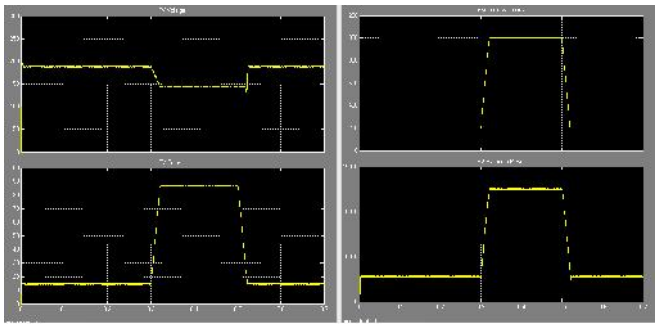

Fig 6 waveforms of MPPT tracking performance

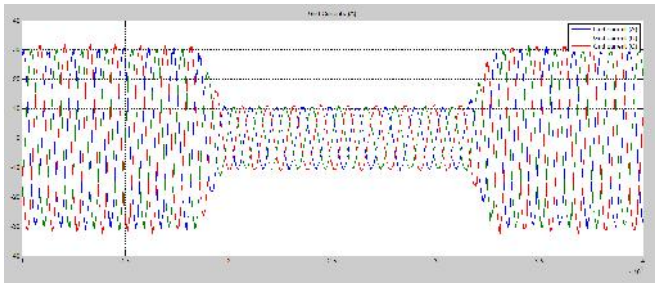

Fig 7 measured grid currents

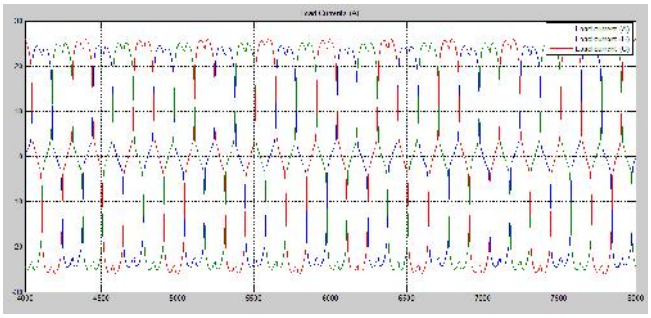

Fig 8 measured load currents

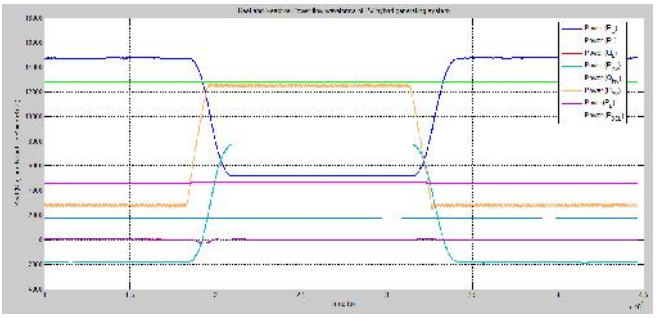

Fig 12 waveforms of all measured powers

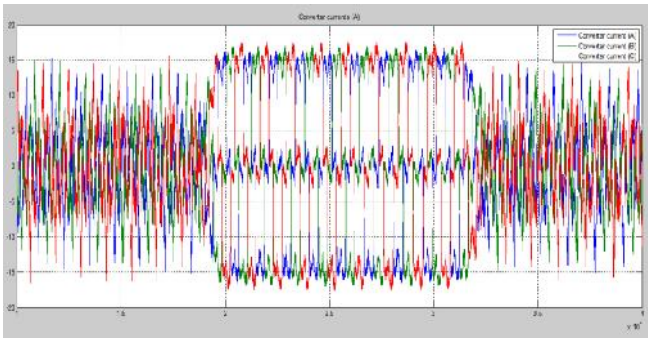

Fig 9 proposed converter currents

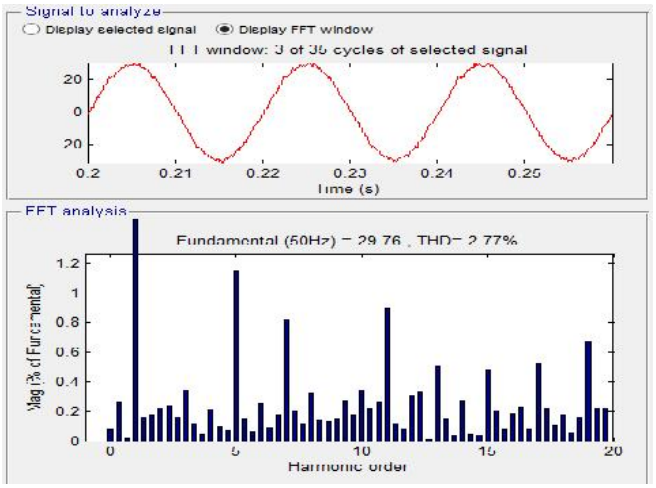

Fig 13 grid current %THD with PI controller

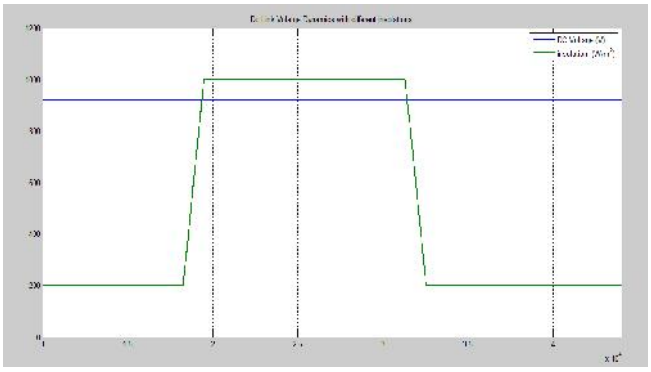

Fig 10 DC link voltages with insolation

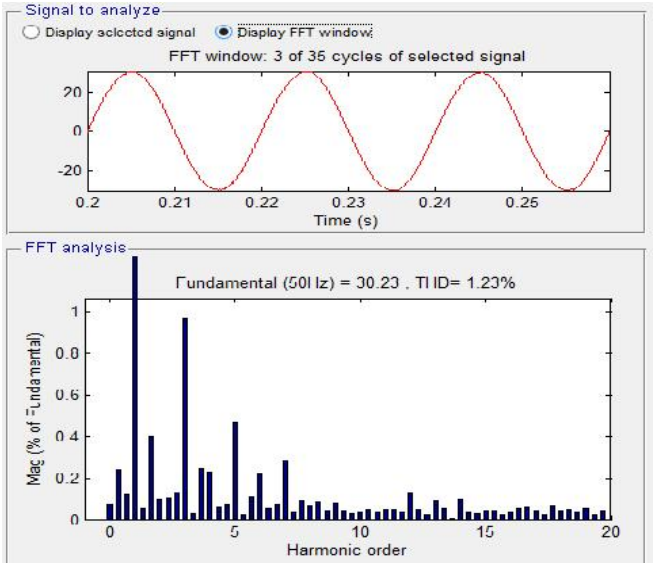

Fig 14 grid current %THD with fuzzy controller

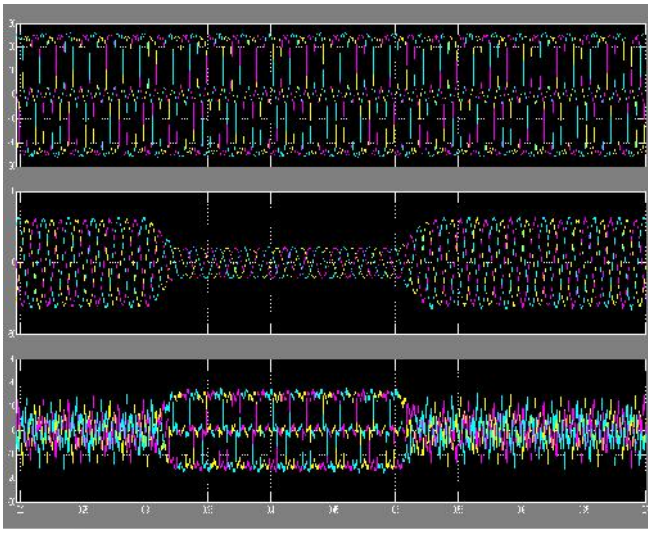

Fig 11 waveforms of all measured currents

CONCLUSIONS

The performance of PV/Battery hybrid energy conversion system has been demonstrated with the application of modified instantaneous symmetrical components theory to μG-VSC proposed in this paper, an efficient control strategy is also proposed for battery converter to regulate the dc bus voltage tightly, under varying solar insolation and dc load conditions. HGICB

converter topology is used to track the MPPT with high gain and less current ripple. The μG-VSC is able to inject the generated power into the grid along with harmonic and reactive power compensation for unbalanced non-linear load at the PCC simultaneously. The system works satisfactorily under dynamic conditions. The simulation results under a unbalanced non-linear load with current THD confirm that the μG-VSC can effectively inject the generated active power along with power quality improvement features and thus, it maintains a sinusoidal and UPF current at the grid side. The THD result shows the fuzzy controller will improves the performance compared with the conventional controller.

REFERENCES

[1] J. Carrasco, L. Franquelo, J. Bialasiewicz, E. Galvan, R. Guisado, M. Prats, J. Leon, and N. Moreno-Alfonso, ―Power-electronic systems for the grid integration of renewable energy sources: A survey,‖ *IEEE Trans. Ind. Electron.*, vol. 53, no. 4, pp. 1002 – 1016, Jun. 2006.

[2] M. de Brito, L. Galotto, L. Sampaio, G. de Azevedo e Melo, and C. Canesin, ―Evaluation of the main mppt techniques for photovoltaic applications,‖ *IEEE Trans. Ind. Electron.*, vol. 60, no. 3, pp. 1156 – 1167, Mar. 2013.

[3] B. Subudhi and R. Pradhan, ―A comparative study on maximum power point tracking techniques for photovoltaic power systems,‖ *IEEE Trans. Sustain. Energy*, vol. PP, no. 99, pp. 1 –10, Mar. 2012.

[4] W. Li and X. He, ―Review of nonisolated high-step-up dc/dc converters in photovoltaic grid-connected applications,‖ *IEEE Trans. Ind. Electron.*, vol. 58, no. 4, pp. 1239 –1250, Apr. 2011.

[5] J. Rocabert, A. Luna, F. Blaabjerg, and P. Rodri andguez, ―Control of power converters in ac microgrids,‖ *IEEE Trans. Power Electron.*, vol. 27, no. 11, pp. 4734 –4749, Nov. 2012.

[6] R. Kadri, J.-P. Gaubert, and G. Champenois, ―An improved maximum power point tracking for photovoltaic grid-connected inverter based on voltage-oriented control,‖ *IEEE Trans. Ind. Electron.*, vol. 58, no. 1, pp. 66 –75, Jan. 2011.

[7] S. Zhang, K.-J. Tseng, D. Vilathgamuwa, T. Nguyen, and X.-Y. Wang, ―Design of a robust grid interface system for pmsg-based wind turbine generators,‖ *IEEE Trans. Ind. Electron.*, vol. 58, no. 1, pp. 316–328, Jan. 2011.

[8] A. Chatterjee, A. Keyhani, and D. Kapoor, ―Identification of photovoltaic source models,‖ *IEEE Trans. Energy Convers.*, vol. 26, no. 3, pp. 883 –889, Sept. 2011.

[9] A. Rahimi, G. Williamson, and A. Emadi, ―Loop-cancellation technique: A novel nonlinear feedback to overcome the destabilizing effect of constant-power loads,‖ *IEEE Trans. Veh. Technol.*, vol. 59, no. 2, pp. 650 –661, Feb. 2010.

[10] A. Radwan and Y. Mohamed, ―Modeling, analysis, and stabilization of converter-fed ac microgrids with high penetration of converterinterfaced loads,‖ *IEEE Trans. Smart Grid.*, vol. 3, no. 3, pp. 1213 – 1225, Sept. 2012.

[11] W. Tang, F. Lee, and R. Ridley, ―Small-signal modeling of average currentmode control,‖ *IEEE Trans. Power Electron.*, vol. 8, no. 2, pp. 112 –119, Apr. 1993.